Editors' Suggestion | Featured in Physics

Time-Integrated Neutrino Source Searches with 10 Years of IceCube Data

M. G. Aartsen,[16] M. Ackermann,[55] J. Adams,[16] J. A. Aguilar,[12] M. Ahlers,[20] M. Ahrens,[46] C. Alispach,[26] K. Andeen,[37] T. Anderson,[52] I. Ansseau,[12] G. Anton,[24] C. Argüelles,[14] J. Auffenberg,[1] S. Axani,[14] P. Backes,[1] H. Bagherpour,[16] X. Bai,[43] A. Balagopal,[29] A. Barbano,[26] S. W. Barwick,[28] B. Bastian,[55] V. Baum,[36] S. Baur,[12] R. Bay,[8] J. J. Beatty,[18,19] K.-H. Becker,[54] J. Becker Tjus,[11] S. BenZvi,[45] D. Berley,[17] E. Bernardini,[55] D. Z. Besson,[30] G. Binder,[8,9] D. Bindig,[54] E. Blaufuss,[17] S. Blot,[55] C. Bohm,[46] M. Börner,[21] S. Böser,[36] O. Botner,[53] J. Böttcher,[1] E. Bourbeau,[20] J. Bourbeau,[35] F. Bradascio,[55] J. Braun,[35] S. Bron,[26] J. Brostean-Kaiser,[55] A. Burgman,[53] J. Buscher,[1] R. S. Busse,[38] T. Carver,[26,*] C. Chen,[6] E. Cheung,[17] D. Chirkin,[35] S. Choi,[48] K. Clark,[31] L. Classen,[38] A. Coleman,[39] G. H. Collin,[14] J. M. Conrad,[14] P. Coppin,[13] P. Correa,[13] D. F. Cowen,[51,52] R. Cross,[45] P. Dave,[6] C. De Clercq,[13] J. J. DeLaunay,[52] H. Dembinski,[39] K. Deoskar,[46] S. De Ridder,[27] P. Desiati,[35] K. D. de Vries,[13] G. de Wasseige,[13] M. de With,[10] T. DeYoung,[22] A. Diaz,[14] J. C. Díaz-Vélez,[35] H. Dujmovic,[29] M. Dunkman,[52] E. Dvorak,[43] B. Eberhardt,[35] T. Ehrhardt,[36] P. Eller,[52] R. Engel,[29] P. A. Evenson,[39] S. Fahey,[35] A. R. Fazely,[7] J. Felde,[17] K. Filimonov,[8] C. Finley,[46] D. Fox,[51] A. Franckowiak,[55] E. Friedman,[17] A. Fritz,[36] T. K. Gaisser,[39] J. Gallagher,[34] E. Ganster,[1] S. Garrappa,[55] L. Gerhardt,[9] K. Ghorbani,[35] T. Glauch,[25] T. Glüsenkamp,[24] A. Goldschmidt,[9] J. G. Gonzalez,[39] D. Grant,[22] Z. Griffith,[35] S. Griswold,[45] M. Günder,[1] M. Gündüz,[11] C. Haack,[1] A. Hallgren,[53] R. Halliday,[22] L. Halve,[1] F. Halzen,[35] K. Hanson,[35] A. Haungs,[29] D. Hebecker,[10] D. Heereman,[12] P. Heix,[1] K. Helbing,[54] R. Hellauer,[17] F. Henningsen,[25] S. Hickford,[54] J. Hignight,[23] G. C. Hill,[2] K. D. Hoffman,[17] R. Hoffmann,[54] T. Hoinka,[21] B. Hokanson-Fasig,[35] K. Hoshina,[35] F. Huang,[52] M. Huber,[25] T. Huber,[29,55] K. Hultqvist,[46] M. Hünnefeld,[21] R. Hussain,[35] S. In,[48] N. Iovine,[12] A. Ishihara,[15] G. S. Japaridze,[5] M. Jeong,[48] K. Jero,[35] B. J. P. Jones,[4] F. Jonske,[1] R. Joppe,[1] D. Kang,[29] W. Kang,[48] A. Kappes,[38] D. Kappesser,[36] T. Karg,[55] M. Karl,[25] A. Karle,[35] U. Katz,[24] M. Kauer,[35] J. L. Kelley,[35] A. Kheirandish,[35] J. Kim,[48] T. Kintscher,[55] J. Kiryluk,[47] T. Kittler,[24] S. R. Klein,[8,9] R. Koirala,[39] H. Kolanoski,[10] L. Köpke,[36] C. Kopper,[22] S. Kopper,[50] D. J. Koskinen,[20] M. Kowalski,[10,55] K. Krings,[25] G. Krückl,[36] N. Kulacz,[23] N. Kurahashi,[42] A. Kyriacou,[2] M. Labare,[27] J. L. Lanfranchi,[52] M. J. Larson,[17] F. Lauber,[54] J. P. Lazar,[35] K. Leonard,[35] A. Leszczyńska,[29] M. Leuermann,[1] Q. R. Liu,[35] E. Lohfink,[36] C. J. Lozano Mariscal,[38] L. Lu,[15] F. Lucarelli,[26] J. Lünemann,[13] W. Luszczak,[35] Y. Lyu,[8,9] W. Y. Ma,[55] J. Madsen,[44] G. Maggi,[13] K. B. M. Mahn,[22] Y. Makino,[15] P. Mallik,[1] K. Mallot,[35] S. Mancina,[35] I. C. Mariş,[12] R. Maruyama,[40] K. Mase,[15] H. S. Matis,[9] R. Maunu,[17] F. McNally,[33] K. Meagher,[35] M. Medici,[20] A. Medina,[19] M. Meier,[21] S. Meighen-Berger,[25] T. Menne,[21] G. Merino,[35] T. Meures,[12] J. Micallef,[22] D. Mockler,[12] G. Momenté,[36] T. Montaruli,[26] R. W. Moore,[23] R. Morse,[35] M. Moulai,[14] P. Muth,[1] R. Nagai,[15] U. Naumann,[54] G. Neer,[22] H. Niederhausen,[25] M. U. Nisa,[22] S. C. Nowicki,[22] D. R. Nygren,[9] A. Obertacke Pollmann,[54] M. Oehler,[29] A. Olivas,[17] A. O'Murchadha,[12] E. O'Sullivan,[46] T. Palczewski,[8,9] H. Pandya,[39] D. V. Pankova,[52] N. Park,[35] P. Peiffer,[36] C. Pérez de los Heros,[53] S. Philippen,[1] D. Pieloth,[21] E. Pinat,[12] A. Pizzuto,[35] M. Plum,[37] A. Porcelli,[27] P. B. Price,[8] G. T. Przybylski,[9] C. Raab,[12] A. Raissi,[16] M. Rameez,[20] L. Rauch,[55] K. Rawlins,[3] I. C. Rea,[25] R. Reimann,[1] B. Relethford,[42] M. Renschler,[29] G. Renzi,[12] E. Resconi,[25] W. Rhode,[21] M. Richman,[42] S. Robertson,[9] M. Rongen,[1] C. Rott,[48] T. Ruhe,[21] D. Ryckbosch,[27] D. Rysewyk,[22] I. Safa,[35] S. E. Sanchez Herrera,[22] A. Sandrock,[21] J. Sandroos,[36] M. Santander,[50] S. Sarkar,[41] S. Sarkar,[23] K. Satalecka,[55] M. Schaufel,[1] H. Schieler,[29] P. Schlunder,[21] T. Schmidt,[17] A. Schneider,[35] J. Schneider,[24] F. G. Schröder,[29,39] L. Schumacher,[1] S. Sclafani,[42] D. Seckel,[39] S. Seunarine,[44] S. Shefali,[1] M. Silva,[35] R. Snihur,[35] J. Soedingrekso,[21] D. Soldin,[39] M. Song,[17] G. M. Spiczak,[44] C. Spiering,[55] J. Stachurska,[55] M. Stamatikos,[19] T. Stanev,[39] R. Stein,[55] P. Steinmüller,[29] J. Stettner,[1] A. Steuer,[36] T. Stezelberger,[9] R. G. Stokstad,[9] A. Stößl,[15] N. L. Strotjohann,[55] T. Stürwald,[1] T. Stuttard,[20] G. W. Sullivan,[17] I. Taboada,[6] F. Tenholt,[11] S. Ter-Antonyan,[7] A. Terliuk,[55] S. Tilav,[39] K. Tollefson,[22] L. Tomankova,[11] C. Tönnis,[49] S. Toscano,[12] D. Tosi,[35] A. Trettin,[55] M. Tselengidou,[24] C. F. Tung,[6] A. Turcati,[25] R. Turcotte,[29] C. F. Turley,[52] B. Ty,[35] E. Unger,[53] M. A. Unland Elorrieta,[38] M. Usner,[55] J. Vandenbroucke,[35] W. Van Driessche,[27] D. van Eijk,[35] N. van Eijndhoven,[13] S. Vanheule,[27] J. van Santen,[55] M. Vraeghe,[27] C. Walck,[46] A. Wallace,[2] M. Wallraff,[1] N. Wandkowsky,[35] T. B. Watson,[4] C. Weaver,[23] A. Weindl,[29] M. J. Weiss,[52] J. Weldert,[36] C. Wendt,[35] J. Werthebach,[35] B. J. Whelan,[2] N. Whitehorn,[32] K. Wiebe,[36] C. H. Wiebusch,[1] L. Wille,[35] D. R. Williams,[50] L. Wills,[42] M. Wolf,[25] J. Wood,[35] T. R. Wood,[23] K. Woschnagg,[8] G. Wrede,[24] D. L. Xu,[35] X. W. Xu,[7] Y. Xu,[47] J. P. Yanez,[23] G. Yodh,[28] S. Yoshida,[15] T. Yuan,[35] and M. Zöcklein[1]

[1]*III. Physikalisches Institut, RWTH Aachen University, D-52056 Aachen, Germany*

[2]*Department of Physics, University of Adelaide, Adelaide, 5005, Australia*

[3]*Department of Physics and Astronomy, University of Alaska Anchorage, 3211 Providence Dr., Anchorage, Alaska 99508, USA*

[4]*Department of Physics, University of Texas at Arlington, 502 Yates St., Science Hall Rm 108, Box 19059, Arlington, Texas 76019, USA*

[5]CTSPS, Clark-Atlanta University, Atlanta, Georgia 30314, USA
[6]School of Physics and Center for Relativistic Astrophysics, Georgia Institute of Technology, Atlanta, Georgia 30332, USA
[7]Department of Physics, Southern University, Baton Rouge, Louisiana 70813, USA
[8]Department of Physics, University of California, Berkeley, California 94720, USA
[9]Lawrence Berkeley National Laboratory, Berkeley, California 94720, USA
[10]Institut für Physik, Humboldt-Universität zu Berlin, D-12489 Berlin, Germany
[11]Fakultät für Physik & Astronomie, Ruhr-Universität Bochum, D-44780 Bochum, Germany
[12]Université Libre de Bruxelles, Science Faculty CP230, B-1050 Brussels, Belgium
[13]Vrije Universiteit Brussel (VUB), Dienst ELEM, B-1050 Brussels, Belgium
[14]Department of Physics, Massachusetts Institute of Technology, Cambridge, Massachusetts 02139, USA
[15]Department of Physics and Institute for Global Prominent Research, Chiba University, Chiba 263-8522, Japan
[16]Department of Physics and Astronomy, University of Canterbury, Private Bag 4800, Christchurch, New Zealand
[17]Department of Physics, University of Maryland, College Park, Maryland 20742, USA
[18]Department of Astronomy, Ohio State University, Columbus, Ohio 43210, USA
[19]Department of Physics and Center for Cosmology and Astro-Particle Physics, Ohio State University, Columbus, Ohio 43210, USA
[20]Niels Bohr Institute, University of Copenhagen, DK-2100 Copenhagen, Denmark
[21]Department of Physics, TU Dortmund University, D-44221 Dortmund, Germany
[22]Department of Physics and Astronomy, Michigan State University, East Lansing, Michigan 48824, USA
[23]Department of Physics, University of Alberta, Edmonton, Alberta, Canada T6G 2E1
[24]Erlangen Centre for Astroparticle Physics, Friedrich-Alexander-Universität Erlangen-Nürnberg, D-91058 Erlangen, Germany
[25]Physik-department, Technische Universität München, D-85748 Garching, Germany
[26]Département de physique nucléaire et corpusculaire, Université de Genève, CH-1211 Genève, Switzerland
[27]Department of Physics and Astronomy, University of Gent, B-9000 Gent, Belgium
[28]Department of Physics and Astronomy, University of California, Irvine, California 92697, USA
[29]Karlsruhe Institute of Technology, Institut für Kernphysik, D-76021 Karlsruhe, Germany
[30]Department of Physics and Astronomy, University of Kansas, Lawrence, Kansas 66045, USA
[31]SNOLAB, 1039 Regional Road 24, Creighton Mine 9, Lively, Ontario, Canada P3Y 1N2
[32]Department of Physics and Astronomy, UCLA, Los Angeles, California 90095, USA
[33]Department of Physics, Mercer University, Macon, Georgia 31207-0001, USA
[34]Department of Astronomy, University of Wisconsin, Madison, Wisconsin 53706, USA
[35]Department of Physics and Wisconsin IceCube Particle Astrophysics Center, University of Wisconsin, Madison, Wisconsin 53706, USA
[36]Institute of Physics, University of Mainz, Staudinger Weg 7, D-55099 Mainz, Germany
[37]Department of Physics, Marquette University, Milwaukee, Wisconsin, 53201, USA
[38]Institut für Kernphysik, Westfälische Wilhelms-Universität Münster, D-48149 Münster, Germany
[39]Bartol Research Institute and Department of Physics and Astronomy, University of Delaware, Newark, Delaware 19716, USA
[40]Department of Physics, Yale University, New Haven, Connecticut 06520, USA
[41]Department of Physics, University of Oxford, Parks Road, Oxford OX1 3PU, United Kingdom
[42]Department of Physics, Drexel University, 3141 Chestnut Street, Philadelphia, Pennsylvania 19104, USA
[43]Physics Department, South Dakota School of Mines and Technology, Rapid City, South Dakota 57701, USA
[44]Department of Physics, University of Wisconsin, River Falls, Wisconsin 54022, USA
[45]Department of Physics and Astronomy, University of Rochester, Rochester, New York 14627, USA
[46]Oskar Klein Centre and Department of Physics, Stockholm University, SE-10691 Stockholm, Sweden
[47]Department of Physics and Astronomy, Stony Brook University, Stony Brook, New York 11794-3800, USA
[48]Department of Physics, Sungkyunkwan University, Suwon 16419, Korea
[49]Institute of Basic Science, Sungkyunkwan University, Suwon 16419, Korea
[50]Department of Physics and Astronomy, University of Alabama, Tuscaloosa, Alabama 35487, USA
[51]Department of Astronomy and Astrophysics, Pennsylvania State University, University Park, Pennsylvania 16802, USA
[52]Department of Physics, Pennsylvania State University, University Park, Pennsylvania 16802, USA
[53]Department of Physics and Astronomy, Uppsala University, Box 516, S-75120 Uppsala, Sweden
[54]Department of Physics, University of Wuppertal, D-42119 Wuppertal, Germany
[55]DESY, D-15738 Zeuthen, Germany

(Received 18 October 2019; revised manuscript received 13 December 2019; accepted 6 January 2020; published 6 February 2020)

This Letter presents the results from pointlike neutrino source searches using ten years of IceCube data collected between April 6, 2008 and July 10, 2018. We evaluate the significance of an astrophysical signal from a pointlike source looking for an excess of clustered neutrino events with energies typically above ~1 TeV among the background of atmospheric muons and neutrinos. We perform a full-sky scan, a search within a selected source catalog, a catalog population study, and three stacked Galactic catalog searches.

The most significant point in the northern hemisphere from scanning the sky is coincident with the Seyfert II galaxy NGC 1068, which was included in the source catalog search. The excess at the coordinates of NGC 1068 is inconsistent with background expectations at the level of 2.9σ after accounting for statistical trials from the entire catalog. The combination of this result along with excesses observed at the coordinates of three other sources, including TXS $0506+056$, suggests that, collectively, correlations with sources in the northern catalog are inconsistent with background at 3.3σ significance. The southern catalog is consistent with background. These results, all based on searches for a cumulative neutrino signal integrated over the 10 years of available data, motivate further study of these and similar sources, including time-dependent analyses, multimessenger correlations, and the possibility of stronger evidence with coming upgrades to the detector.

DOI: 10.1103/PhysRevLett.124.051103

Cosmic rays (CRs) have been observed for over a hundred years [1] penetrating the entire surface of the Earth's atmosphere in the form of leptonic and hadronic charged particles with energies up to $\sim 10^{20}$ eV [2]. These particles are heavily deflected on their journey to the Earth by magnetic fields and, although at energies $\gtrsim 10^{19}$ eV this deflection could become much smaller, their origin is still largely unknown. Very-high-energy (VHE) γ rays ($E_\gamma > 100$ GeV) travel without deflection and so provide evidence for astrophysical acceleration sites. However, these photons can be produced by both leptonic and hadronic processes and are attenuated by extragalactic background light, meaning they cannot probe redshifts larger than $z \sim 1$ at energies above ~ 1 TeV. In comparison, only hadronic processes can produce an astrophysical neutrino flux which would travel unattenuated and undeflected from the source to the Earth. Thus, astrophysical neutrino observations are critical to identify CR sources, or to discover distant very-high-energy accelerators.

IceCube has discovered a flux of astrophysical neutrinos in multiple diffuse searches [3–6], which integrate observed emission over most of the sky. Notably, a potential neutrino source, TXS $0506+056$, has been identified through a multimessenger campaign around a high-energy IceCube event in September 2017 [7]. IceCube also found evidence for neutrino emission over ~ 110 days from 2014–2015 at the location of TXS $0506+056$ when examining over nine years of archival data [8]. Nonetheless, the estimated flux from this source alone is less than 1% of the total astrophysical neutrino flux [3] and the contribution of a catalog of blazars as a population to the best fit total astrophysical neutrino flux between 10 TeV and 2 PeV is limited to 27% [9]. In this Letter we search for various pointlike neutrino sources using 10 years of IceCube observations.

The IceCube neutrino telescope is a cubic kilometer array of digital optical modules (DOMs) each containing a 10" PMT [10] and on-board read-out electronics [11]. These DOMs are arranged in 86 strings between 1.45 and 2.45 km below the surface of the ice at the South Pole [12]. The DOMs are sensitive to Cherenkov light from energy losses of ultrarelativistic charged particles traversing the ice. This analysis targets astrophysical muon neutrinos and antineutrinos (ν_μ), which undergo charged-current interactions in the ice to produce a muon traversing the detector. The majority of the background for this analysis originates from CRs interacting with the atmosphere to produce showers of particles including atmospheric muons and neutrinos. The atmospheric muons from the southern hemisphere are able to penetrate the ice and are detected as tracklike events in IceCube at a rate orders of magnitude higher than the corresponding atmospheric neutrinos [12]. Almost all of the atmospheric muons from the northern hemisphere are filtered out by the Earth. However, poorly reconstructed atmospheric muons from the southern sky create a significant background in the northern hemisphere. Atmospheric neutrinos also produce muons from charged-current ν_μ interactions, acting as an irreducible background in both hemispheres. Neutral-current interactions or ν_e and ν_τ charged-current interactions produce particle showers with spherical topology known as cascade events. Tracks at $\sim$TeV energies are reconstructed with a typical angular resolution of $\lesssim 1°$, while cascades have an angular resolution of $\sim 10°$–$15°$ [13]. This analysis selects tracklike events because of their better angular resolution. Tracks have the additional advantage that they can be used even if the neutrino interaction vertex is located outside of the detector. This greatly increases the detection efficiency.

During the first three years of data included here, IceCube was incomplete and functioned with 40, 59, and 79 strings. For these years and also during the first year of data taking of the full detector (IC86), the event selection and reconstruction was updated until it stabilized in 2012, as detailed in Table I. Seven years of tracks were previously analyzed to search for point sources [14]. Subsequently, an eight-year sample of tracks from the northern sky used for diffuse muon neutrino searches was also analyzed looking for point sources [15]. The aim of this Letter is to introduce a selection which unifies the event filtering adopted in these two past searches. Additionally, the direction reconstruction [16,17] has been updated to use the deposited event energy in the detector. This improves

TABLE I. IceCube configuration, livetime, number of final tracklike events, start and end date and published reference in which the sample selection is described.

Data samples					
Year	Livetime (Days)	Number of events	Start day	End day	Ref.
IC40	376.4	36900	2008/04/06	2009/05/20	[19]
IC59	352.6	107011	2009/05/20	2010/05/31	[20]
IC79	316.0	93133	2010/06/01	2011/05/13	[21]
IC86-2011	332.9	136244	2011/05/13	2012/05/15	[22]
IC86-2012-18	2198.2	760923	2012/04/26 [a]	2018/07/10	This Letter

[a]Start date for test runs of the new processing. The remainder of this run began 2012/05/15.

the angular resolution by more than 10% for events above 10 TeV compared to the seven-year study [14], and achieves a similar angular resolution as the eight-year northern diffuse track selection [15], which also uses deposited event energy in the direction reconstruction (see Fig. 1). The absolute pointing accuracy of IceCube by combining many events has been demonstrated to be $\lesssim 0.2°$ [18] via measurements of the effect of the Moon shadow on the background CR flux.

Different criteria are applied to select track-like events from the northern and southern hemisphere (with a boundary between them at declination $\delta = -5°$), because the background differs in these two regions. Almost all the atmospheric muons in the northern hemisphere can be removed by selecting high-quality tracklike events. In the southern hemisphere, the atmospheric background is reduced by strict cuts on the reconstruction quality and minimum energy deposited in the detector, since the astrophysical neutrino fluxes are expected to have a harder energy spectrum than the background of atmospheric muons and neutrinos. This effectively removes almost all

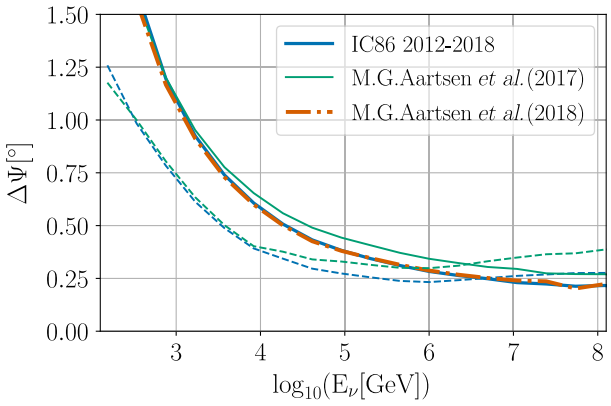

FIG. 1. The median angle between simulated neutrino and reconstructed muon directions as a function of energy for the data selection used in the latest six years compared to that in Ref. [14] (solid and dashed lines are for northern and southern hemispheres, respectively) and in Ref. [15] for the northern hemisphere. The differences between hemispheres come from the differences in the background composition and the respective selection criteria.

southern hemisphere events with an estimated energy below ~10 TeV [23].

In both hemispheres, atmospheric muons and cascade events are further filtered using multivariate boosted decision trees (BDTs). In this analysis, a single BDT is trained to recognize three classes of events in the northern hemisphere: single muon tracks from atmospheric and astrophysical neutrinos, atmospheric muons, and cascades, where neutrino-induced tracks are treated as signal. This BDT uses 11 variables related to event topology and reconstruction quality. When applied to simulated events, the northern BDT preserves ~90% of the atmospheric neutrinos and ~0.1% of the atmospheric muons from the initial selection of tracklike events, also applied in previous muon neutrino searches [14,15]. In the southern hemisphere, the BDT and selection filters are taken from Ref. [14]. The final all-sky event rate of ~2 mHz is dominated by muons from atmospheric neutrinos in the northern hemisphere and by high-energy, well-reconstructed muons in the southern hemisphere. This updated selection applied to the final six years of data shown in Table I. The preceding four years of data are handled exactly as in the past.

The point-source searches conducted in this paper use the existing maximum-likelihood ratio method which compares the hypothesis of pointlike signal plus diffuse background versus a background-only null hypothesis. All of the searches and source catalogs were predefined before any of the following results were obtained. This technique, described in Refs. [19,30], was also applied in the seven- and eight-year point source searches [14,15]. The all-sky scan and the selected source catalog searches look for directions which maximize the likelihood-ratio in the northern and southern hemisphere separately. Since this analysis assumes pointlike sources, it is suboptimal to those with extended neutrino emission regions. The sensitivity of this analysis to a neutrino flux with an E^{-2} spectrum, calculated according to [19], shows a ~35% improvement compared to the seven-year all-sky search [14] due to the longer livetime, updated event selection, and updated reconstructions. While the sensitivity in the northern hemisphere is comparable to the eight-year study for an E^{-2} spectrum [15], the analysis presented in this work achieves

a ∼30% improvement in sensitivity to sources with a softer spectrum, such as E^{-3}. This difference is due to the more general nature of this work which assumes an $E^{-\gamma}$ power-law energy spectrum, where $1 \leq \gamma \leq 4$, whereas the eight-year study targets the sources responsible for the diffuse astrophysical neutrino flux seen in [31] by applying a strict Gaussian prior on the spectral index, γ, centered at 2.19 ± 0.1.

All-sky scan.—The brightest sources of astrophysical neutrinos may differ from the brightest sources observed in the electromagnetic (EM) spectrum. For example, cosmic accelerators can be surrounded by a dense medium which attenuates photon emission while neutrinos could be further generated by cosmic-ray interactions in the medium. For this reason, a general all-sky search for the brightest single pointlike neutrino source in each hemisphere is conducted, and is unbiased by EM observations. This involves maximizing the signal-over-background likelihood-ratio at a grid of points across the entire sky with a finer spacing ($\sim 0.1° \times \sim 0.1°$) than the typical event angular uncertainty. The points within 8° of the celestial poles are excluded due to poor statistics and limitations in the background estimation technique.

At each position on the grid, the likelihood-ratio function is maximized resulting in a maximum test-statistic (TS), a best fit number of astrophysical neutrino events ($\hat{n}_s$), and the spectral index ($\hat{\gamma}$) for an assumed power-law energy spectrum. The local pretrial probability (p-value) of obtaining the given or larger TS value at a certain location from only background is estimated at every grid point by fitting the TS distribution from many background trials with a χ^2 function. Each background trial is obtained from the data themselves by scrambling the right ascension of each event, thereby removing any clustering of the signal. The location of the most significant p-value in each hemisphere is defined to be the hottest spot. The post-trial probability is estimated by comparing the p-value of the hottest spot in the data with a distribution of hottest spots in the corresponding hemisphere from a large number of background trials.

The most significant point in the northern hemisphere is found at equatorial coordinates (J2000) right ascension 40.9°, declination −0.3° with a local p-value of 3.5×10^{-7}. The best fit parameters at this spot are $\hat{n}_s = 61.5$ and $\hat{\gamma} = 3.4$. Considering the trials from examining the entire hemisphere increases the p-value to 9.9×10^{-2} post-trial. The probability skymap in a 3° by 3° window around the most significant point in the northern hemisphere is plotted in Fig. 2. This point is found 0.35° from the active galaxy NGC 1068, which is independently included as a source in the northern source catalog. To study whether the 0.35° offset between the all-sky hotspot and NGC 1068 is typical of the reconstruction uncertainty of a neutrino source, we inject a soft-spectrum source according to the best-fit $E^{-3.2}$ flux at the *Fermi*-LAT coordinates for NGC 1068 into our

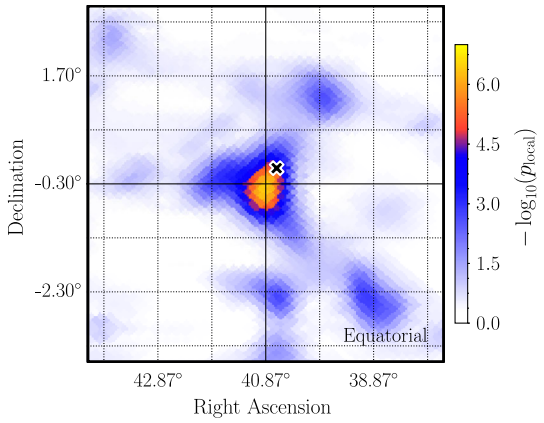

FIG. 2. Local pre-trial p-value map around the most significant point in the Northern hemisphere. The black cross marks the coordinates of the galaxy NGC 1068 taken from *Fermi*-4FGL.

background samples. Scanning in a 5° window around the injection point, we find that the median separation between the most significant hotspot and the injection point is 0.35°. Thus, if the excess is due to an astrophysical signal from NGC 1068, the offset between the all-sky hotspot and *Fermi*-LAT's coordinates is consistent with the IceCube angular resolution for such a source.

The most significant hotspot in the southern hemisphere, at right ascension 350.2° and declination-56.5°, is less significant with a pretrial p-value of 4.3×10^{-6} and fit parameters $\hat{n}_s = 17.8$, and $\hat{\gamma} = 3.3$. The p-value of this hotspot becomes 0.75 post-trial. Both hotspots alone are consistent with a background-only hypothesis.

Source catalog searches.—The motivation of this search is to improve sensitivity to detect possible neutrino sources already observed in γ rays. A new catalog composed of 110 sources has been constructed which updates the catalog used in previous sources searches [14]. The new catalog uses the latest γ ray observations and is based on rigorous application of a few simple criteria, described below. The size of the catalog was chosen to limit the trials factor applied to the most significant source in the catalog such that a 5σ significance before trials would remain above 4σ after trials. These 110 sources are composed of Galactic and extragalactic sources, which are selected separately.

The extragalactic sources are selected from the *Fermi*-LAT 4FGL catalog [32] since it provides the highest-energy unbiased measurements of γ-ray sources over the full sky. Sources from 4FGL are weighted according to the integral *Fermi*-LAT flux above 1 GeV divided by the sensitivity flux for this analysis at the respective source declination. The 5% highest-weighted BL Lacs and flat spectrum radio quasars (FSRQs) are each selected. The minimum weighted integral flux from the combined selection of BL Lac and FSRQs is used as a flux threshold to include sources marked as unidentified blazars and AGN. Eight 4FGL sources are identified as starburst galaxies. Since these types of objects are thought to host hadronic emission

[33,34], they are all included in the final source list. The blazar TXS 0506 + 056 is selected in the top 5% of BL Lacs due to its high luminosity in γ rays and its location in the most sensitive region of the sky for IceCube.

To select Galactic sources, we consider measurements of VHE γ-ray sources from TeVCat [35,36] and gammaCat [37]. Spectra of the γ rays were converted to equivalent neutrino fluxes, assuming a purely hadronic origin of the observed γ-ray emission where $E_\gamma \simeq 2E_\nu$, and compared to the sensitivity of this analysis at the declination of the source (Fig. 3). Those Galactic objects with predicted energy fluxes $> 50\%$ of IceCube's sensitivity limit for an E^{-2} spectrum, were included in the source catalog. A total of 12 Galactic γ-ray sources survived the selection.

The final list of neutrino source candidates is a northern-sky catalog containing 97 objects (87 extragalactic and 10 Galactic) and a southern-sky catalog containing 13 sources (11 extragalactic and 2 Galactic). The large north-south difference is due to the difference in the sensitivity of IceCube in the northern and southern hemispheres. The post-trial p-value for each catalog describes the significance of the single most significant source in the catalog and is calculated as the fraction of background trials where the pre-trial p-value of the most significant fluctuation is smaller than the pre-trial p-value found in data.

The obtained pre-trial p-values are provided in the supplementary material and their associated 90% C.L. flux upper limits are shown in Fig. 3, together with the expected sensitivity and discovery potential fluxes. The most significant excess in the northern catalog of 97 sources is found in the direction of the galaxy NGC 1068, analyzed for the first time by IceCube in this analysis, with a local pre-trial p-value of 1.8×10^{-5} (4.1σ). The best fit parameters are $\gamma = 3.2$ and $\hat{n}_s = 50.4$, consistent with the results for the all-sky northern hottest spot, 0.35° away. From Fig. 2 it can be inferred that the significance of the all-sky hotspot and the excess at NGC 1068 are dominated by the same cluster of events. The parameters of the best fit spectrum at the coordinates of NGC 1068 are shown in Fig. 4. When the significance of NGC 1068 is compared to the most significant excesses in the northern catalog from many background trials, the post-trial significance is 2.9σ.

Out of the 13 different source locations examined in the Southern catalog, the most significant excess has a pretrial p-value of 0.06 in the direction of PKS 2233-148. The associated post-trial p-value is 0.55, which is consistent with background.

Four sources in the northern catalog found a pretrial p-value < 0.01: NGC 1068, TXS 0506 + 056, PKS 1424 + 240, and GB6 J1542 + 6129. Evidence has been presented for TXS 0506 + 056 to be a neutrino source [8] using an overlapping event selection in a time-dependent analysis. However, TXS 0506 + 056 was included in the northern catalog independently of this result due to its relatively high γ-ray flux observed by *Fermi*-LAT. In this Letter, in which we only consider the cumulative signal integrated over 10 years, we find a pretrial significance of 3.6σ at the coordinates of TXS 0506 + 056 for a best fit spectrum of $E^{-2.1}$, consistent with previous results.

In addition to the single source search, a source population study is conducted to understand if excesses from several sources, each not yet at evidence level, can cumulatively indicate a population of neutrino sources in the catalog.

The population study uses the pretrial p-values of each source in the catalog and searches for an excess in the

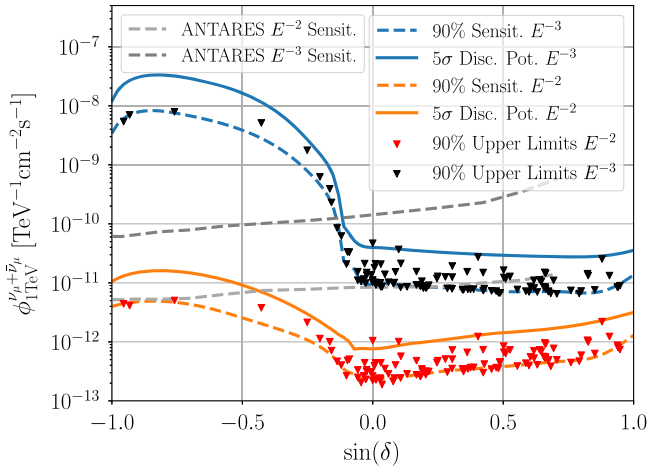

FIG. 3. 90% C.L. median sensitivity and 5σ discovery potential as a function of source declination for a neutrino source with an E^{-2} and E^{-3} spectrum. The 90% upper limits are shown excluding an E^{-2} and E^{-3} source spectrum for the sources in the source list. The grey curves show the 90% C.L. median sensitivity from 11 yrs of ANTARES data [38].

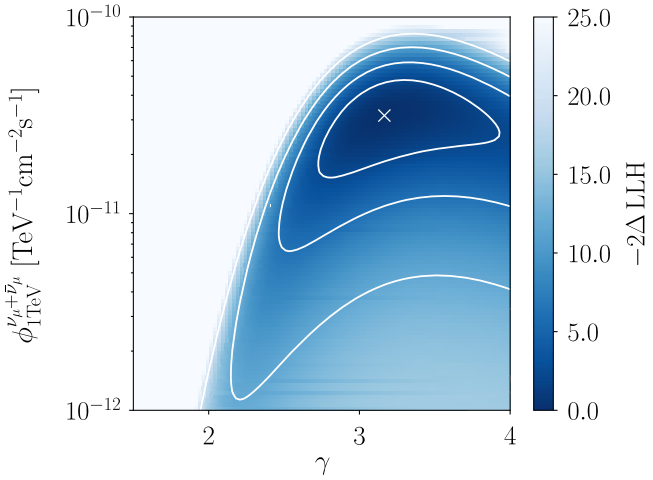

FIG. 4. Likelihood map at the position of NGC 1068 as a function of the astrophysical flux spectral index and normalization at 1 TeV. Contours show 1, 2, 3, and 4σ confidence intervals assuming Wilks' theorem with 2 degrees of freedom [39]. The best fit spectrum is point marked with "×".

number of small p-values compared to the uniform background expectation. If the number of objects in the search catalog is N, and the number of sources below a given threshold p_k is k, then the probability of background producing k or more sources with p-values smaller than p_k is given by the cumulative binomial probability:

$$p_{\mathrm{bkg}} = \sum_{i=k}^{N} P_{\mathrm{binom}}(i|p_k, N) = \sum_{i=k}^{N} \binom{N}{i} p_k^i (1-p_k)^{N-i}. \tag{1}$$

In order to maximize sensitivity to any possible population size of neutrino sources within the catalog, the probability threshold (p_k) is increased iteratively to vary k between 1 and N. The result of this search is the most significant p_{bkg} from N different tested values of k, then the post-trial p-value from this search must take into account a trial factor for the different tested values of k.

The most significant p_{bkg} from the northern catalog population analysis is 3.3×10^{-5} (4.0σ), which is found when $k = 4$. The four most significant sources which contribute to this excess are those with p-value < 0.01 as described above. When accounting for the fact that different signal population sizes are tested, the post-trial p-value is 4.8×10^{-4} (3.3σ). Since evidence has already been presented for TXS $0506 + 056$ to be a neutrino source [8], an *a posteriori* search is conducted removing this source from the catalog. The resulting most significant excess is 2.3σ post-trial due to the remaining three most significant sources. For the southern catalog, the pretrial p-value of the most significant excess is 0.12, provided by 5 of the 13 sources. The resulting post-trial p-value is 0.36.

Stacked source searches.—In the case of catalogs of sources that produce similar fluxes, stacking searches require a lower flux per source for a discovery than considering each source individually. Three catalogs of Galactic γ-ray sources are stacked in this paper. Sources are selected from VHE γ-ray measurements and categorized into pulsar wind nebulae (PWN), supernova remnants (SNR), and unidentified objects (UNID), with the aim of grouping objects likely to have similar properties as Galactic neutrino emitters. The final groups consist of 33 PWN, 23 SNR, and 58 UNID described in the Supplemental Material. A weighting scheme is adopted to describe the relative contribution expected from each source in a single catalog based on the integral of the extrapolated γ-ray flux above 10 TeV. All three catalogs find p-values > 0.1.

Conclusion.—This Letter presents an updated event selection optimized for pointlike neutrino source signals applied to 10 years of IceCube data taken from April 2008 to July 2018. Multiple neutrino source searches are performed: an all-sky scan, a source catalog and corresponding catalog population study for each hemisphere, and three stacked Galactic-source searches.

TABLE II. Summary of final p-values (pretrial and post-trial) for each pointlike source search implemented in this Letter.

Analysis	Category	Pretrial significance (p_{local})	Post-trial significance
All-Sky Scan	North	3.5×10^{-7}	9.9×10^{-2}
	South	4.3×10^{-6}	0.75
Source list	North	1.8×10^{-5}	2.0×10^{-3} (2.9σ)
	South	5.9×10^{-2}	0.55
Catalog	North	3.3×10^{-5}	4.8×10^{-4} (3.3σ)
Population	South	0.12	0.36
Stacking Search	SNR	…	0.11
	PWN	…	1.0
	UNID	…	0.4

The results of these analyses, all searching for cumulative neutrino signals integrated over the 10 years of data-taking, are summarized in Table II. The most significant source in the northern catalog, NGC 1068, is inconsistent with a background-only hypothesis at 2.9σ due to being located 0.35° from the most significant excess in the northern hemisphere and the northern source catalog provides a 3.3σ inconsistency with a background-only hypothesis for the entire catalog. This result comes from an excess of significant p-values in the directions of the Seyfert II galaxy NGC 1068, the blazar TXS $0506 + 056$, and the BL Lacs PKS $1424 + 240$ and GB6 J1542 + 6129. NGC 1068, at a 14.4 Mpc distance, is the most luminous Seyfert II galaxy detected by *Fermi*-LAT [24]. NGC 1068 is an observed particle accelerator, charged particles are accelerated in the jet of the AGN or in the AGN-driven molecular wind [40], producing γ rays and potentially neutrinos. Other work has previously indicated NGC 1068 as a potential CR accelerator [33,41,42]. Assuming that the observed excess is indeed of astrophysical origin and connected with NGC 1068, the best-fit neutrino spectrum inferred from this work is significantly higher than that predicted from models developed to explain the *Fermi*-LAT gamma-ray measurements [25]. However, the large uncertainty from our spectral measurement and the high x-ray and γ-ray absorption along the line of sight [26,43] prevent a straight forward connection. Time-dependent analyses and the possibility of correlating with multimessenger observations for this and other sources may provide additional evidence of neutrino emission and insights into its origin. Continued data-taking, more refined event reconstruction, and the planned upgrade of IceCube promise further improvements in sensitivity [44].

The authors gratefully acknowledge the support from the following agencies and institutions: USA: U.S. National Science Foundation-Office of Polar Programs,

U.S. National Science Foundation-Physics Division, Wisconsin Alumni Research Foundation, Center for High Throughput Computing (CHTC) at the University of Wisconsin-Madison, Open Science Grid (OSG), Extreme Science and Engineering Discovery Environment (XSEDE), U.S. Department of Energy-National Energy Research Scientific Computing Center, Particle astrophysics research computing center at the University of Maryland, Institute for Cyber-Enabled Research at Michigan State University, and Astroparticle physics computational facility at Marquette University; Belgium: Funds for Scientific Research (FRS-FNRS and FWO), FWO Odysseus and Big Science programmes, and Belgian Federal Science Policy Office (Belspo); Germany: Bundesministerium für Bildung und Forschung (BMBF), Deutsche Forschungsgemeinschaft (DFG), Helmholtz Alliance for Astroparticle Physics (HAP), Initiative and Networking Fund of the Helmholtz Association, Deutsches Elektronen Synchrotron (DESY), and High Performance Computing cluster of the RWTH Aachen; Sweden: Swedish Research Council, Swedish Polar Research Secretariat, Swedish National Infrastructure for Computing (SNIC), and Knut and Alice Wallenberg Foundation; Australia: Australian Research Council; Canada: Natural Sciences and Engineering Research Council of Canada, Calcul Québec, Compute Ontario, Canada Foundation for Innovation, WestGrid, and Compute Canada; Denmark:Villum Fonden, Danish National Research Foundation (DNRF), Carlsberg Foundation; New Zealand: Marsden Fund; Japan: Japan Society for Promotion of Science (JSPS) and Institute for Global Prominent Research (IGPR) of Chiba University; Korea: National Research Foundation of Korea (NRF); Switzerland: Swiss National Science Foundation (SNSF); United Kingdom: Department of Physics, University of Oxford.

*Corresponding author.
analysis@icecube.wisc.edu

[1] V. F. Hess, Über Beobachtungen der durchdringenden Strahlung bei sieben Freiballonfahrten, Phys. Z. **13**, 1084 (1912).
[2] D. J. Bird *et al.*, Detection of a cosmic ray with measured energy well beyond the expected spectral cutoff due to cosmic microwave radiation, Astrophys. J. **441**, 144 (1995).
[3] M. G. Aartsen *et al.* (IceCube Collaboration), Observation and characterization of a cosmic muon neutrino flux from the Northern hemisphere using six years of IceCube data, Astrophys. J. **833**, 3 (2016).
[4] M. G. Aartsen *et al.* (IceCube Collaboration), The IceCube neutrino observatory—Contributions to ICRC 2017 Part II: Properties of the atmospheric and astrophysical neutrino flux, Proc. Sci. ICR2017 (**2017**) 981 [arXiv:1710.01191].
[5] M. Aartsen *et al.*, Evidence for high-energy extraterrestrial neutrinos at the IceCube detector, Science **342**, 1242856 (2013).
[6] M. G. Aartsen *et al.* (IceCube Collaboration), Observation of High-Energy Astrophysical Neutrinos in Three Years of IceCube Data, Phys. Rev. Lett. **113**, 101101 (2014).
[7] M. G. Aartsen *et al.*, Multimessenger observations of a flaring blazar coincident with high-energy neutrino Icecube-170922a, Science **361**, eaat1378 (2018).
[8] M. G. Aartsen *et al.* (IceCube Collaboration), Neutrino emission from the direction of the blazar TXS 0506 + 056 prior to the IceCube-170922A alert, Science **361**, 147 (2018).
[9] M. G. Aartsen *et al.* (IceCube Collaboration), The contribution of Fermi-2LAC blazars to the diffuse TeV-PeV neutrino flux, Astrophys. J. **835**, 45 (2017).
[10] R. Abbasi *et al.*, Calibration and characterization of the IceCube photomultiplier tube, Nucl. Instrum. Methods Phys. Res., Sect. A **618**, 139 (2010).
[11] R. Abbasi *et al.* (IceCube Collaboration), The IceCube data acquisition system: Signal capture, digitization, and time-stamping, Nucl. Instrum. Methods Phys. Res., Sect. A **601**, 294 (2009).
[12] M. G. Aartsen *et al.* (IceCube Collaboration), The IceCube Neutrino observatory: Instrumentation and online systems, J. Instrum. **12**, P03012 (2017).
[13] M. G. Aartsen *et al.* (IceCube Collaboration), Search for astrophysical sources of neutrinos using cascade events in IceCube, Astrophys. J. **846**, 136 (2017).
[14] M. G. Aartsen *et al.* (IceCube Collaboration), All-sky search for time-integrated neutrino emission from astrophysical sources with 7 yr of IceCube data, Astrophys. J. **835**, 151 (2017).
[15] M. G. Aartsen *et al.* (IceCube Collaboration), Search for steady point-like sources in the astrophysical muon neutrino flux with 8 years of IceCube data, Eur. Phys. J. C. **79**, 234 (2018).
[16] J. Ahrens *et al.* (AMANDA Collaboration), Muon track reconstruction and data selection techniques in AMANDA, Nucl. Instrum. Methods Phys. Res., Sect. A **524**, 169 (2004).
[17] M. G. Aartsen *et al.*, Improvement in fast particle track reconstruction with robust statistics, Nucl. Instrum. Methods Phys. Res., Sect. A **736**, 143 (2014).
[18] M. G. Aartsen *et al.* (IceCube Collaboration), Observation of the cosmic-ray shadow of the Moon with IceCube, Phys. Rev. D **89**, 102004 (2014).
[19] R. Abbasi *et al.* (IceCube Collaboration), Time-integrated searches for point-like sources of neutrinos with the 40-string IceCube detector, Astrophys. J. **732**, 18 (2011).
[20] M. G. Aartsen *et al.* (IceCube Collaboration), Search for time-independent neutrino emission from astrophysical sources with 3 yr of IceCube data, Astrophys. J. **779**, 132 (2013).
[21] K. Schatto, Stacked searches for high-energy neutrinos from blazars with IceCube, Ph. D. thesis, Mainz U., 2014.
[22] M. G. Aartsen *et al.* (IceCube Collaboration), Searches for extended and point-like neutrino sources with four years of IceCube data, Astrophys. J. **796**, 109 (2014).
[23] See Supplemental Material at http://link.aps.org/supplemental/10.1103/PhysRevLett.124.051103 for more details on the properties of the event selection, catalogs of investigated astrophysical sources, further context for the observations around NGC 1068. This material includes Refs. [24–29].

[24] M. Ackermann *et al.*, GeV observations of star-forming galaxies with the fermi large area telescope, Astrophys. J. **755**, 164 (2012).
[25] A. Lamastra, F. Fiore, D. Guetta, L. A. Antonelli, S. Colafrancesco, N. Menci, S. Puccetti, A. Stamerra, and L. Zappacosta, Galactic outflow driven by the active nucleus and the origin of the gamma-ray emission in NGC 1068, Astron. Astrophys. **596**, A68 (2016).
[26] A. Lamastra, N. Menci, F. Fiore, L. A. Antonelli, S. Colafrancesco, D. Guetta, and A. Stamerra, Extragalactic gamma-ray background from AGN winds and star-forming galaxies in cosmological galaxy formation models, Astron. Astrophys. **607**, A18 (2017).
[27] T. Neunhoffer, Estimating the angular resolution of tracks in neutrino telescopes based on a likelihood analysis, Astropart. Phys. **25**, 220 (2006).
[28] V. A. Acciari *et al.* (MAGIC Collaboration), Constraints on gamma-ray and neutrino emission from NGC 1068 with the MAGIC telescopes, Astrophys. J. **883**, 135 (2019).
[29] F. Aharonian *et al.* (H.E.S.S. Collaboration), Observations of selected AGN with H.E.S.S, Astron. Astrophys. **441**, 465 (2005).
[30] J. Braun, J. Dumm, F. De Palma, C. Finley, A. Karle, and T. Montaruli, Methods for point source analysis in high energy neutrino telescopes, Astropart. Phys. **29**, 299 (2008).
[31] C. Haack and C. Wiebusch (IceCube Collaboration), A measurement of the diffuse astrophysical muon neutrino flux using eight years of IceCube data, Proc. Sci., ICRC2017 (**2018**) 1005.
[32] The Fermi-LAT Collaboration, Fermi large area telescope fourth source catalog, arXiv:1902.10045.
[33] A. Loeb and E. Waxman, The cumulative background of high energy neutrinos from starburst galaxies, J. Cosmol. Astropart. Phys. 05 (2006) 003.
[34] K. Murase, M. Ahlers, and B. C. Lacki, Testing the hadronuclear origin of PeV neutrinos observed with IceCube, Phys. Rev. D **88**, 121301(R) (2013).
[35] TeVCat: Online catalogue of TeV sources, http://tevcat.uchicago.edu/ (2018).
[36] S. P. Wakely and D. Horan, TeVCat: An online catalog for very high energy gamma-ray astronomy, Int. Cosmic Ray Conf. **3**, 1341 (2008).
[37] GammaCat: Online catalogue of Gamma-ray sources, https://gamma-cat.readthedocs.io/data/overview.html (2018).
[38] J. Aublin, G. Illuminati, and S. Navas (ANTARES Collaboration), Searches for point-like sources of cosmic neutrinos with 11 years of ANTARES data, arXiv:1908.08248.
[39] S. S. Wilks, The large-sample distribution of the likelihood ratio for testing composite hypotheses, Ann. Math. Stat. **9**, 60 (1938).
[40] A. Lamastra, F. Fiore, D. Guetta, L. A. Antonelli, S. Colafrancesco, N. Menci, S. Puccetti, A. Stamerra, and L. Zappacosta, Galactic outflow driven by the active nucleus and the origin of the gamma-ray emission in NGC 1068, Astron. Astrophys. **596**, A68 (2016).
[41] T. M. Yoast-Hull, J. S. Gallagher III, E. G. Zweibel, and J. E. Everett, Active galactic nuclei, neutrinos, and interacting cosmic rays in NGC 253 and NGC 1068, Astrophys. J. **780**, 137 (2014).
[42] B. C. Lacki, T. A. Thompson, E. Quataert, A. Loeb, and E. Waxman, On the GeV & TeV detections of the Starburst galaxies M82 & NGC 253, Astrophys. J. **734**, 107 (2011).
[43] R. Wojaczyński, A. Niedźwiecki, F.-G. Xie, and M. Szanecki, Gamma-ray activity of Seyfert galaxies and constraints on hot accretion flows, Astron. Astrophys. **584**, A20 (2015).
[44] J. van Santen (IceCube Gen2 Collaboration), IceCube-Gen2: The next-generation neutrino observatory for the South Pole, Proc. Sci., ICRC2017 (**2018**) 991.